INTERNATIONAL JOURNAL OF ENERGY RESEARCH

INTERNATIONAL JOURNAL OF ENERGY RESEARCH
Int. J. Energy Res. (2017)
Published online in Wiley Online Library (wileyonlinelibrary.com). DOI: 10.1002/er.3758

Performance of large-scale biomass gasifiers in a biorefinery, a state-of-the-art reference

Alberto Alamia[1,*,†], Anton Larsson[2], Claes Breitholtz[3] and Henrik Thunman[1]

[1]Department of Energy and Environment, Chalmers University of Technology, Gothenburg, Sweden
[2]Göteborg Energi AB, Gothenburg, Sweden
[3]Valmet AB, Gothenburg, Sweden

SUMMARY

The Gothenburg Biomass Gasification plant (2015) is currently the largest plant in the world producing biomethane (20 $MW_{biomethane}$) from woody biomass. We present the experimental data from the first measurement campaign and evaluate the mass and energy balances of the gasification sections at the plant. Measures improving the efficiency including the use of additives (potassium and sulfur), high-temperature pre-heating of the inlet streams, improved insulation of the reactors, drying of the biomass and introduction of electricity as a heat source (power-to-gas) are investigated with simulations. The cold gas efficiency was calculated in 71.7%LHV_{daf} using dried biomass (8% moist). The gasifier reaches high fuel conversion, with char gasification of 54%, and the fraction of the volatiles is converted to methane of 34%$_{mass}$. Because of the design, the heat losses are significant (5.2%LHV_{daf}), which affect the efficiency. The combination of potential improvements can increase the cold gas efficiency to 83.5%LHV_{daf}, which is technically feasible in a commercial plant. The experience gained from the Gothenburg Biomass Gasification plant reveals the strong potential biomass gasification at large scale. © 2017 The Authors. *International Journal of Energy Research* published by John Wiley & Sons Ltd.

KEY WORDS

biomass gasification; GoBiGas; dual fluidized bed; mass balance; power-to-gas; biomethane; SNG

Correspondence

*Alberto Alamia, Department of Energy and Environment, Chalmers University of Technology, Hörsalsvägen 7, S-412 96 Gothenburg, Sweden.

[†]E-mail: alamia@chalmers.se

Received 26 October 2016; Revised 21 March 2017; Accepted 26 March 2017

INTRODUCTION

Societal ambitions to create a circular economy necessitate more sustainable use of our biomass resources [1–4]. In particular, biomass residues, such as stew, bark and branches, can be converted into valuable energy products, in factories that are generally referred to as 'biorefineries'. Both thermochemical and biochemical conversion can be integrated in a biorefinery, although the latter is not particularly efficient at decomposing lignin and hemicellulose, with only thermochemical processes, involving gasification, achieving full conversion of the residues of woody biomass [2,5]. With gasification, the carbon matrix of the lignocellulose is broken down into simple molecules, such as carbon monoxide and hydrogen, which are subsequently synthesised to create high-value biofuels or chemicals. Because of its high efficiency and feedstock flexibility, gasification has been identified as a core process in any circular economy scenario [2,6], and different technologies have been tested over the past decades in several pilot plants [7,8]. However, no industrial unit intended for commercial operation has been built to date.

A first-of-its-kind demonstration plant for the gasification of forest residues on a commercial scale with full downstream synthesis to biofuel was constructed within the Gothenburg Biomass Gasification (GoBiGas) project [9] in Sweden. The GoBiGas plant is the largest plant of its kind and is the first to convert solid biomass to high-quality biomethane, for injection into the national gas grid [9]. The purpose of the GoBiGas project is to establish the performance of the commercial plant and to acquire experience towards the construction of a large-scale (>100 MW) process. For these reasons, the plant is equipped with several measurement points and control options, making the data obtained from GoBiGas the first real reference to support techno-economic analyses and

energy system modelling, both of which have been conducted over the past decades [10–14].

The plant, which is owned by Göteborg Energi (a local utility company that produces heat and power), is designed to target the following high-performance parameters: the production of 20 MW of biomethane, operation for 8000 h/year, ≥65% biomass to biomethane efficiency (η_{bCH4}) and total efficiency (biomass plus district heating) of ≥90%. The total cost to date for the project has been M€165, of which M€24 was provided as governmental support through the Swedish Energy Agency. Table I provides a summary of the investment costs for the different parts of the process, defined according to the main component, where the cost includes all the surrounding systems and equipment of the plant, including scale factors to enable estimation of the costs associated with plants of different scales.

The planning of the GoBiGas project started in May 2005, together with an ambitious research programme funded by the government and industry, which also included the building of a 2–4-MW research gasifier that was commissioned in December 2007 on the campus of Chalmers University of Technology. Construction of the GoBiGas plant started in 2011 and was completed in November 2013, requiring 300 000 man-h of engineering and 800 000 man-h of construction, with an associated labour cost of M€90. The construction of the gasification section was assigned to Valmet AB (former Metso Power), on licence from Repotec GmbH. The subsequent commissioning process took 21 months, during which several major challenges were overcome. Two major breakthroughs occurred during the commissioning phase. First, at 6 months, potassium was added to saturate and stabilise the chemistry that controls the catalytic effect, to assure the quality of the produced gas [15,16], thereby avoiding any clogging of the product gas cooler. Second, the bed height of the gasifier was lowered so that the fuel could be fed closer to the surface of the bubbling bed in the gasifier, thereby reducing the heat transfer and clogging of the fuel-feeding screw and enabling more than 1600 h of continuous operation. At the time of writing, October 2016, the plant is operational and delivers biomethane to the gas grid. Further research is needed to optimise the performance of the plant and improve the efficiency of the process. The present study focuses on establishing the mass and energy balances of the gasification section, so as to evaluate its performance and identify pathways towards optimisation, as well as on creating a reference for the techno-economic and energy system analyses.

Table I. Summary of the costs of the different parts of the process, including the estimated SF, which is defined as *C*/Cref = (*P*/Pref)SF, where *C* is the cost, *P* is the power and 'ref' indicates the values of the reference pant

Part of process	Cost (M€)	Scale factor
Gasifier section (total)	32.8	
Fuel feeding	8.25	0.62
Gasifier	11	0.80
Product gas cooler, filter and scrubber	4.5	0.79
Flue gas cleaning	8.25	0.55
Methanation section (total)	65.5	
Carbon beds	13.7	0.62
Syngas compressor	13.7	0.60
Hydrogenation and sulfur removal	7.2	0.62
Shift and pre-methanation	10	0.62
CO_2 separation	7.2	0.62
Methanation and drying	13.7	0.62
Buildings and construction (total)	21	0.40

SF, scale factor.

A schematic of the GoBiGas biomass-to-biomethane process is shown in Figure 1 (a high-resolution figure is provided in the Supporting Information), in which the plant is presented in a simplified form as two macro-sections: gasification, where the solid fuel is converted to the product gas, and methanation, where the product gas is refined to biomethane. The actual building contains 5000 m^3 of concrete; 800 t of rebar; 1300 t of structural steel; 25 km of piping; 90 km of electric cables; 130 pumps, compressors, fans and conveyers; 200 towers, reactors, heat exchangers, tanks, and vessels; 2500 instruments; and 650 valves [17]. The gasification section comprises an up-scaled version of a dual fluidised bed (DFB) gasification technology, whereby the gasifier has a capacity that is approximately twofold that of the plants in Senden [18], fourfold that of the thermal power plants in Güssing [19] and eightfold that of the gasifier at Chalmers University of Technology. The design of the GoBiGas gasifier is based on the Güssing pilot plant, rather than a downscale version of the commercial combustion units, as is the case, for example, for the gasification system at Chalmers. Nevertheless, the GoBiGas technology shares features with circulating fluidised bed combustors that have an external heat exchanger, which are commercially available at the scale of several hundreds of MW. In this analogy, the circulating bed used as the combustor in the GoBiGas gasifier corresponds to a 10-MW_{th} combustor, and the bubbling bed used as the gasifier corresponds to an external heat recovery unit of around 5 MW_{th}. Building this type of reactor system in small scale is challenging and requires several simplifications that affect efficiency. The methanation section is based on well-proven processes and technologies, which are downscaled to fit the size of the gasification section.

This paper presents the first evaluation of the GoBiGas plant that focuses on the gasification section, because the efficiency of DFB systems limits the performance of the overall biomethane production process. This study uses the results obtained in the first measurement campaign with full operation of the gasifier using wood pellets as the fuel. The evaluation is based on the process parameters extracted from the measurements and incorporated into a simulation, in which the effects of various identified improvements for a commercial-size unit are investigated. The overall scope of the present study is to assess the efficiency of the gasification section in a large-scale plant based on the experience gained from the GoBiGas demonstration plant.

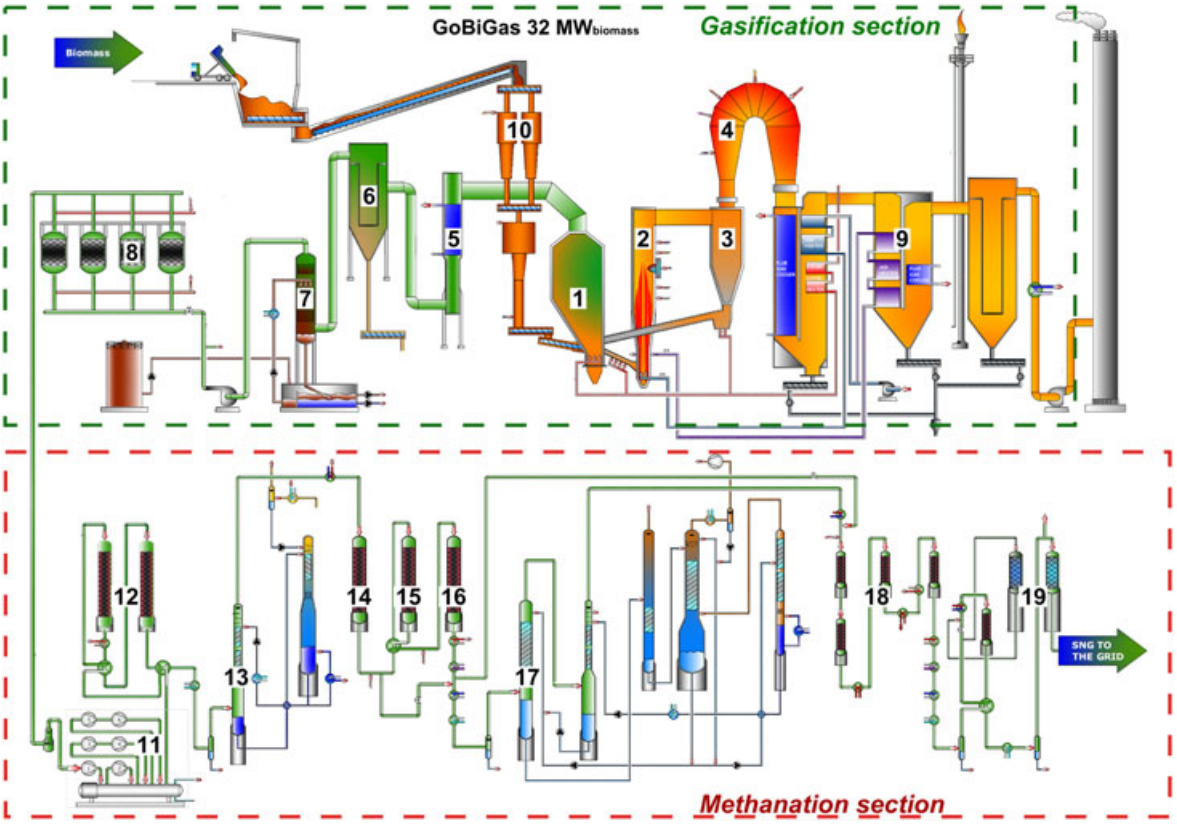

Figure 1. Process schematic of the Gothenburg Biomass Gasification (GoBiGas) biomass to biomethane plant: 1, gasifier; 2, combustion chamber; 3, cyclone; 4, post-combustion chamber; 5, raw gas cooler; 6, raw gas filter; 7, rapeseed methyl ester scrubber; 8, carbon beds; 9, flue gas train; 10, fuel feeding system; 11, product gas compressor; 12, hydration of olefins and COS; 13, H_2S removal; 14, guard bed; 15, water–gas shift reactor; 16, pre-methanation; 17, CO_2 removal, 18, methanation; and 19, drying. [Colour figure can be viewed at wileyonlinelibrary.com]

DESCRIPTION OF THE GOBIGAS PLANT

The GoBiGas plant can be operated with either wood pellets or chipped woody biomass as fuel; wood pellets were used during the commissioning of the plant. The fuel is fed to the gasification reactor (number 1, Figure 1), wherein the major part is converted into gas through devolatilization and partial gasification of the char. The remaining char is transported with the bed material to the combustor (number 2), where it is burnt to produce heat. The transportation of heat between the combustor and the gasifier is achieved through circulation of the bed material.

When biomass is gasified, numerous solid-phase and gas-phase compounds are produced. The distribution and composition of the raw gas depend on the operating conditions, as well as the catalytic activity of the bed material, ash components or additives. DFB gasifiers yield a rather high percentage of methane already in the produced raw gas (6–12% vol.) [20,21] because of the relatively low operating temperature of <900 °C. When the target product is biomethane, this is one of the major advantages of the DFB process over other gasification technologies, which are operated at higher temperatures. Because using a low temperature for the process can lead to a significant level of tar, limiting the tar yield becomes a major challenge with the DFB technique. A common approach to limiting the tar yield is to use an active bed material [21–23], thereby avoiding fouling or deactivation in the downstream equipment [24–26].

Olivine is a natural magnesium-iron-silicate ore that is commonly used as the bed material in DFB gasifiers because of its ability to reduce the yield of tar and its tendency not to agglomerate at these process temperature levels [15,23,27,28]. However, to achieve the desired catalytic behaviour, olivine needs to be activated. There are different approaches to activate olivine; the one used in the GoBiGas plant is based on the addition of potassium [15,28,29].

A continuous flow of fresh rapeseed methyl ester (RME) (0.03–0.035 MW_{RME}/MW_{fuel}) is fed to the scrubber to avoid saturation of tar, especially naphthalene, which can be problematic as it crystallises when the RME is saturated. The used RME and the extracted tar are fed to the combustion side of the gasifier for destruction and heat recovery. After the scrubber (P3), there remains mainly

light cyclic hydrocarbons, such as benzene, toluene and xylene (referred to as BTX), and a small fraction of the naphthalene, as well as trace amounts of larger tar components. As the slip of tar is proportional to the volume of fresh scrubbing liquid, there is a trade-off between avoiding the slip and minimising the use of scrubbing liquid. Downstream of the scrubber, a fan increases the pressure of the gas, enabling the re-circulation of part of the product gas to the combustor, which is necessary to fulfil the heat demand of the DFB system.

At this point (P3), the quality of the product gas is sufficiently high to be used in several applications, for example, internal combustion engines. However, further cleaning is required for synthetic applications. In brief, the remaining BTX and tar components are removed in a series of three fixed beds that are filled with activated carbon. The plant has four active carbon beds, enabling regeneration of one bed at all times using steam. Currently, the off gases from the regeneration are introduced into the post-combustion chamber for destruction and heat recovery. However, a system is being developed that will allow condensation of the steam and recovery of the tar compounds, which then can be fed to the combustor. The product gas that exits the gasification section (P4) is compressed to 16 bar before it undergoes further cleaning and synthetic steps in the methanation section, which include hydration of olefins and COS (number 12, Figure 1); H_2S removal (13); passage through the guard bed for removal of trace components (14); water–gas shift reaction (15); pre-methanation (16); CO_2 removal (17); four-stage methanation (18); drying (19); and final compression to 30 bar before feeding into the natural gas grid.

Experimental data

For this work, the data were collected at the end of the commissioning period, during which wood pellets were used as the fuel, with the aim of evaluating the performance of the gasification section. The locations of the measurements points in the process are shown as points 1–10 (P1–10) in Figure 2, and the type of measurement that was performed at each point is listed in Table II. The evaluation is based on one operational point with 90% load (wood pellets, 8% moisture) and potassium carbonate (K_2CO_3) as the activation agent [15,28,30], corresponding to ~0.2 kg/t wood pellets. This results in a tar concentration that is below the operability threshold of the plant (around 35 g/Nm [3] dry gas, including BTX and heavy tars). This is the base case in the evaluation and is hereinafter referred to as the *K-activated* (*K-act*) case. The composition of the used wood pellets is given in the Supporting Information (Table S1), and the major operating parameters are summarised in Table III, while the gas and tar measurements are listed in Tables IV and V. The fuel flow to the gasifier (P6 in Figure 2) was calculated based on the carbon balance of the gasification section (P4 and P5) and compared with the scale measurement of the ingoing fuel (Table S1). To simplify the evaluation of the gasification section, the fuel feed was purged with nitrogen (CO_2 produced in the methanation section was used during normal operation, and the methanation section and regeneration of the active carbon beds were not operated to simplify the carbon balance).

MEASURES TO IMPROVE THE EFFICIENCY OF THE DUAL FLUIDISED BED GASIFICATION PROCESS

As described previously, GoBiGas is a demonstration plant for the DFB technology, and the design is not yet optimised for maximum performance in terms of efficiency and availability. Because of the relatively small scale of the demonstration plant and the previous knowledge gap (now filled with the construction of the plant), several measures have been identified to improve the process towards the creation of a commercial plant. The measures evaluated in this work focus on improving the efficiency of the gasification section.

Improvements based on the heat demand of the Gothenburg Biomass Gasification gasifier

The efficiency of a gasification process correlates strongly with the heat demands of the process. The impact on the gasification performance of reducing the total heat demand through different practical measures was assessed. The measures that yielded the greatest effect on the total heat demand were identified as the level of pre-heating of the steam and combustion air; the moisture content of the fuel; heat losses; and the operational temperature. Furthermore, part of the total heat demand could be covered by an additional heat source, such as electricity, as a power-to-gas concept.

The steam used to fluidise the gasifier and the air for the combustor are pre-heated by heat recovery in the flue gas train; during the evaluation, both streams were heated to about 350 °C. Both streams could in principle be heated to a higher temperature, either by heat recovery at elevated higher temperature in the flue gas train or by the addition of an additional heat source. Based on the choice of material, the maximum temperature investigated is 550 °C, which is feasible using steel with material number 1.4401 (3016L). An even higher temperature would increase the material costs considerably and is therefore not considered. Note that in the absence of an additional heat source, the maximum temperature is instead restricted by the temperature of the super heaters that recover the heat from the flue gas train.

The wood pellets used as fuel in the present work have moisture contents of about 8%. However, wood pellets

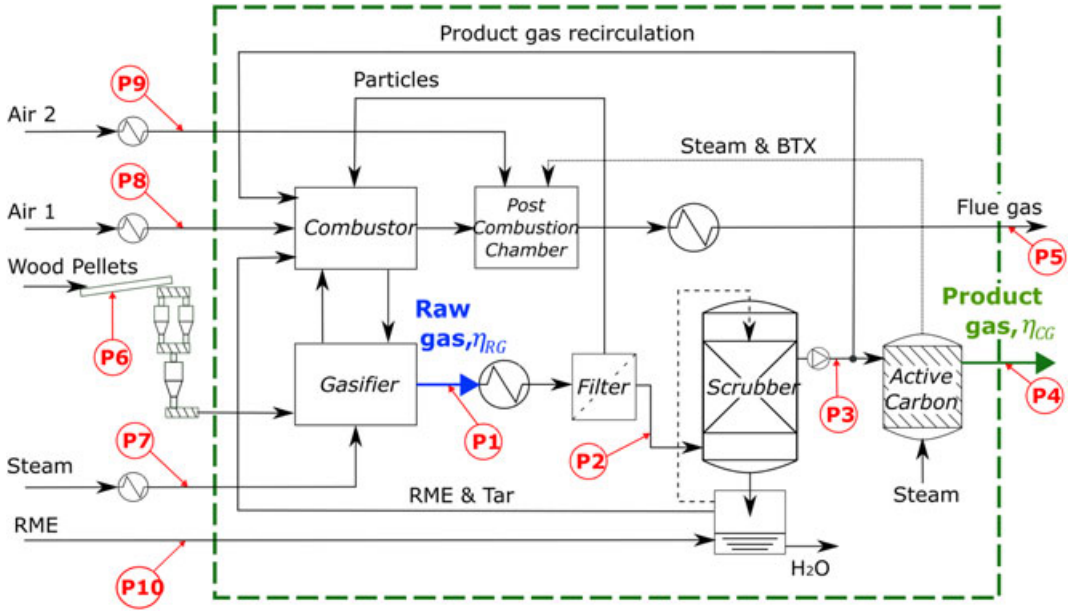

Figure 2. Schematic of the gasification section showing measurement points P1–P10. RME, rapeseed methyl ester; BTX, benzene, toluene and xylene. [Colour figure can be viewed at wileyonlinelibrary.com]

represent a pre-processed fuel, which is more expensive than other biomass-based fuels, such as wood chips or forest residues. To improve the economics of the plant, it is, therefore, relevant to consider fresh biomass that is not pre-treated and has a moisture content of up to 40%. As a higher moisture content is deleterious to process efficiency, a moisture content >40% is not relevant for gasification, at least without the introduction of dryers upstream of the gasifier. Drying on-site is certainly beneficial and can be achieved by exploiting the excess heat in the process. Several drying concepts are available [31], with low-temperature drying (with air and steam) being more suited for integration. For steam gasification, extended drying with recovery of the moisture as gasification media is of interest [32], as this confers dual benefits in terms of drying and pre-evaporation of the gasification steam. The maximum size of the fuel particle is limited by the feeding system to 7–10 cm.

The heat losses are here calculated as the differences in sensible and chemical energy between the inlets and outlets of the DFB gasifier. The heat losses of the GoBiGas plant are higher than those of a regular biomass boiler owing to the small size and the design of the insulation walls (Figure S2). The reactors do not have heat transfer panels coupled to insulation blocks, which would allow control of the temperature of the gas sealing (outer steel lagging), which needs to be higher than the condensation temperature at atmospheric pressure, so as to avoid condensation and corrosion. Instead, the external walls are designed to be cooled by the surrounding air in the building housing the gasifier, where temperatures as high as 140 °C have been measured. As a consequence, there are significant heat losses. Nevertheless, the heat insulation can be easily improved in a large-scale plant using a conventional reactor wall design for commercial fluidised bed combustors.

Table II. Measurements made in the gasification section

Sampling point – sample type	Measured compound(s)	Type of measurement
P1 – hot raw gas	Tar	SPA, temperature
P2 – particle-free gas	Tar	SPA
P3 – cold gas	Tar and permanent gases	NDIR, flow and SPA
P4 – product gas	Permanent gases	GC
P5 – flue gas	Permanent gases	FTIR, flow, temperature and pressure
P6 – fuel feed	Proximate and ultimate analysis	Moisture (offline) and composition (offline)
P7 – steam feed	Steam	Flow, temperature and pressure
P8 – air feed	Air	Flow, temperature and pressure
P9 – air feed	Air	Flow, temperature and pressure
P10 – RME	RME	Flow and heating value (offline)

RME, rapeseed methyl ester; SPA, solid phase adsorption method; NDIR, nondispersive infrared; FTIR, Fourier transform infrared spectroscopy.

Table III. Operational parameters

Operational parameter	Mean	SD
Gasifier bed temperature (°C)	870	2
Raw gas temperature (°C)	815	2
Combustor temperature (°C)	920	3
Steam temperature (°C)	345	14
Air temperature (°C)	348	10
Flue gas temperature (°C)	140	2
Fluidisation steam (Nm^3/h)	4255	53
Combustion air* (Nm^3/h)	8830	109
Post-combustion air (Nm^3/h)	1709	164
Flue gas (Nm^3/h)	13 049	491
Fresh rapeseed methyl ester flow (kg/h)	100	2
Fuel feeding (kg_{daf}/h)†	5820	142

*Including the fluidisation air.
†Calculated form carbon balance.

While the temperature of the gasification section is important for the eventual quality of the gas, it also has a strong impact on the total heat demand of the gasifier.

This creates a trade-off whereby a lower temperature leads to a lower quality gas with higher tar yield, which at the same time enables higher efficiency. With improved catalysis in the gasifier, the temperature can be decreased while retaining the quality of the gas, thereby improving efficiency. During the experiments presented in the present study, the GoBiGas gasifier was operated with a temperature of the gasifier of 870 °C using potassium (K) as the activation additive. As described in previous studies, the addition of sulfur increases further the catalytic effect of potassium, decreasing the tar yield substantially [28,33–35] and decreasing the risk of corrosion [36]. Initial tests have shown that with sulfur addition, the temperature of the gasifier can be decrease to 820 °C while retaining gas quality (as assessed by CH_4 concentration). Therefore, a case with an operating temperature of the gasifier of 820 °C was investigated, to illustrate the potential of decreasing the temperature and, thereby, the heat demand of the process.

To date, the gasifier was operated for more than 8000 h with potassium addition including 5000 h with sulfur addition, without sings of corrosion in the reactors and heat exchangers.

Electricity that can be produced in a steam cycle that recovers the excess heat from the plant is estimated to be in the range of 3–10% of the energy of the dry fuel [10,37–39], while consumption is in the range of 3–5% [9,10,39]. The electricity can be sold to the grid or re-used as a heat source for the gasifier to enhance biomethane production. The simplest way to introduce electricity into the gasification section is through either direct heating of the reactors or further pre-heating of the inlet streams. Introducing a power-to-gas technology makes the gasification process suitable for the storage of renewable electricity from intermittent energy sources (wind and solar) in the form of biomethane.

Case study – performance of a commercial-scale dual fluidised bed gasifier

To understand the potential performance of a commercial-scale DFB gasifier, a case study based on the measures described previously in Improvements based on the heat demand of the Gothenburg Biomass Gasification gasifier section was conducted. The notations and descriptions of the different cases are summarised in Table VI, where the different improvements incorporated in each case are indicated. In the base case potassium is used as activation additive in the GoBiGas gasifier (referred to as *K-act*, in contrast to the *K,S-act* notation, which refers to both *K* and *S* being used as additives). For the *K,S-act* case, the measurements reveal a different gas composition and a reduction in the level of tar, as compared with the *K-act*

Table IV. Permanent gas measurements

	P3		P4		P5	
	Mean	SD	Mean	SD	Mean	SD
H_2 ($vol\%_{dry}$)	39.9	0.49	42.1	0.49	–	–
CO ($vol\%_{dry}$)	24.0	0.3	24.6	0.3	0.02	0.02
CO_2 ($vol\%_{dry}$)	19.9	0.21	18.3	0.21	11.53	1.23
CH_4 ($vol\%_{dry}$)	8.6	0.12	6.8	0.12	–	–
C_2H_2 ($vol\%_{dry}$)	0.13	0.00	0.13	0.00	–	–
C_2H_4 ($vol\%_{dry}$)	2.0	0.07	2.0	0.07	–	–
C_2H_6 ($vol\%_{dry}$)	0.19	0.01	0.19	0.01	–	–
C_3H_6 ($vol\%_{dry}$)	0.001	0.00	0.01	0.00	–	–
N_2 ($vol\%_{dry}$)	5.28‡	0.81	4.0‡	0.81	56.9	5.35
H_2O (vol%)	6.33	–	14.1†	–	27.2	2.55
O_2 (vol%)	–	–	–	–	4.35	1.20
Flow ($Nm^‡/h$)	7998†	9	7157†	6	13 049	491

*Dry flow.
†Saturated.
‡From purge gas.

Table V. Tar measurements

	P1		P3		P4	
	Mean	SD	Mean	SD	Mean	SD
Tar, including BTX (g/Nm^3)	20.5	0.5	13.3	0.3	–	–
Tar, excluding BTX (g/Nm^3)	7.8	0.2	0.7	0.0	–	–
H/C$_{total\ tar}$ (mol/mol)	0.92	–	0.99	–	–	–
O/C$_{total\ tar}$ (mol/mol)	3/10^4	–	5/10^4	–	–	–
H/C$_{BTX}$ (mol/mol)	0.99	–	0.99	–	–	–
O/C$_{BTX}$ (mol/mol)	5/10^4	–	5/10^4	–	–	–
Flow (Nm^3/h)	7998*	9	7998*	9	7157*	6

BTX, benzene, toluene and xylene.
*Dry flow.

Table VI. Designs investigated in the simulation of the gasifier

	K-act	*K,S-act*	*K,S-act LT*	*K,S-act LT, PH, Ql*	*K,S-act LT, PH, Ql, El*	*K,S-act LT, PH, Ql, El$_{int}$*
Activation with *K*	x					
Activation with *K* and *S*		x	x	x	x	x
Low gasification temperature (820 °C)			x	x	x	x
Pre-heating of air and steam to 550 °C				x	x	x
Minimised heat loss				x	x	x
Power-to-gas from the grid					x	
Power-to-gas from excess heat						x

case. The increased catalytic effect achieved through the use of both *K* and *S* could be used to reduce the operating temperature instead of further improving the gas quality and decreasing the tar concentration. When the gasification temperature is reduced to 820 °C (referred to as the *K,S-act LT* case), the resulting gas composition and tar level (Table IX) are assumed to be equal to those in the *K-act* case, albeit with the benefit of a lower heat demand in the reactors. Further improvement to the design are invstegated, such as improved pre-heating of the inlet streams to 550 °C (denoted as case *PH*), reduction of the heat losses to 33% of the original (*Ql*), adding externally produced electricity (*El*) and adding internally produced electricity (*El$_{int}$*), with both of the latter corresponding to 3% of the energy in the fuel. All the cases were investigated for a plant that used dried biomass (8% moisture w.b.) and for a plant that used fresh biomass (40% moisture w.b.).

METHODOLOGY

A black-box model of the mass and energy balances, based on a stochastic analysis of the measurements, is used to calculate a set of key performance parameters that describe the fuel conversion, the efficiency of the process and the levels of uncertainty. The methodology applied has been described previously [40] and is briefly summarised in Mass balance and statistical analysis of the experimental data section.

Key performance parameters

The overall performance of the DFB gasifier is assessed using a set of five efficiencies, calculated using the lower heating value (LHV) on dry ash-free fuel (Table VII). The following three efficiencies are defined based on the energy content of the fuel, E_f: (1) the raw gas efficiency (η_{RG}); (2) the cold gas efficiency (η_{CG}); and (3) the biomethane efficiency (η_{bCH4}) (as defined by Eqs. (1)-(3) in Table VII). The raw gas efficiency represents the energy of the raw gas from the gasifier (including tar) and is a direct measure of the fuel conversion in the gasification reactor (P1 in Figure 2). The cold gas efficiency includes only the permanent gases that exit the gasification section, excluding

Table VII. Definitions based on the LHV of dry ash-free biomass to describe the efficiencies of the η_{RG}, raw gas; η_{CG}, cold gas; η_{bCH4}, biomethane; μ_{sect}, gasification section; η_{plant}, plant; and η_{P2G}, power-to-gas

$$\eta_{RG} = \frac{E_{RG}}{E_f}[\%\mathrm{LHV_{daf}}] \quad (1)$$

$$\eta_{CG} = \frac{E_{CG}}{E_f}[\%\mathrm{LHV_{daf}}] \quad (2)$$

$$\eta_{bCH4} = \frac{E_{bCH4}}{E_f}[\%\mathrm{LHV_{daf}}] \quad (3)$$

$$\eta_{sect} = \frac{E_{CG}}{E_f + E_{RME} + El}[\%E_{tot}] \quad (4)$$

$$\eta_{plant} = \frac{E_{bCH4}}{E_f + E_{RME} + El_{tot}}[\%E_{tot}] \quad (5)$$

$$\eta_{P2G} = \frac{E_{bCH4} - E'_{bCH4}}{El_{sect}}[\mathrm{MW_{bCH4}/MW_{el}}] \quad (6)$$

LHV, lower heating value.

Table VIII. Fuel conversion reactions [40]: R1, devolatilisation; R2, gasification; R3, syngas combustion; R4, volatile conversion; R5, volatile combustion; and R6, char combustion

$\sum Z_i + \lambda_v = 1 - Y_{ch}$	(R1)
$(\dot{X}_g - \lambda_{ch}) \cdot [(n_C,\ n_H, n_O)_{ch} + d_1 \cdot H_2O \quad \rightarrow\ a_1 \cdot CO + b_1 \cdot H_2]$	(R2)
$\lambda_{ch} \cdot \left[(n_C,\ n_H, n_O)_{ch} + d_2 \cdot H_2O + \overline{n}_{O,ch} \rightarrow a_2 \cdot CO_2 + b_2 \cdot H_2O\right]$	(R3)
$Z_i \cdot [(n_C,\ n_H, n_O)_v \rightarrow\ a_{3,i} \cdot CO_2 + b_{3,i} \cdot H_2O + c_{3,i} \cdot C_{p,i}H_{q,i}O_{k,i}]$	(R4)
$\lambda_v \cdot \left[(n_C,\ n_H, n_O)_v + \overline{n}_{O,v} \rightarrow a_4 \cdot CO_2 + b_4 \cdot H_2O\right]$	(R5)
$(1 - X_g) \cdot \left[(n_C,\ n_H, n_O)_{ch} + \lambda_a \cdot \overline{n}_{O,f} \rightarrow a_5\ CO_2 + b_5\ H_2O + \overline{n}_{O,f} \cdot \lambda_{Otr} + \overline{n}_{O,f} \cdot \left(\lambda_a - \lambda_{Otr} - \frac{\overline{n}_{O,ch}}{\overline{n}_{O,f}}\right)\right]$	(R6)

the tar and BTX, and the re-circulated product gas, which are separated and fed to the combustor (P4). The biomethane efficiency represents the amount of energy in the fuel that is retained in the final biomethane product (theoretical, as described later). The biomethane efficiency is also the value used for the performance target of the GoBiGas project and is set at $\eta_{bCH4} > 65\%LHV_{daf}$. Two additional efficiencies are defined to assess the overall performance of the gasification section (η_{sect} in Eq. (4), Table VII) and of the whole plant (η_{plant} in Eq. (5), Table VII); all the energy inputs (biomass, RME and electricity) are included in the calculation. The biomethane and plant efficiencies are based on the assumption that the conversion from product gas to biomethane follows the general conversion reaction:

$$(n_C,\ n_H, n_O)_{PG} \rightarrow a \cdot CH_4 + b \cdot CO_2 + c \cdot H_2O. \qquad (1)$$

Based on (1), around 85% of the energy in the cold gas measured at P4 can be retained as biomethane. Furthermore, electricity used for the operation of the plant, including the intermediate and final compression stages, is estimated at $3.75\%LHV_{daf}$, which is included in the plant efficiency.

Unlike other power-to-gas processes, the power-to-methane conversion in the plant cannot be assessed only by an efficiency that is defined as the increase in biomethane production in relation to the electricity input, because the feedstock that is converted has a high energy value. Instead, the power-to-methane efficiency is set as being equal to the plant efficiency (Eq. (5), Table VII). The power-to-gas efficiency of the power-to-methane process (η_{P2G} in Eq. (6), Table VII) is used to assess the electricity conversion to biomethane based on the reference production, E^*_{bCH4}.

Mass balance and statistical analysis of the experimental data

The validity of the calculated variables reflects the quality and completeness of the measurements themselves. Therefore, a statistical analysis is used to assess the uncertainty of the calculated variables by establishing a synthetic dataset ($>10^6$ cases) that is based on the uncertainty of the measurements, assuming a normal distribution for all the variables [41]. Systematic errors, such as incomplete characterisation of the raw gas compounds or errors in the measurements, are not included because they are unknown. The overall mass and energy balances are assessed with a black-box approach to handle the high degree of complexity of the reactions in the gasification process and the high degree of freedom in the operation of the double-reactor system. The mass balance is used to estimate three types of fuel conversion variables, which are calculated from the measurements: (1) the degree of char-gasified X_g (Eq. (B1)); (2) oxygen transport by the bed material between the combustion and the gasification side of the gasifier λ_{Otr} (Eq. (B3)); and the fraction of volatile matter that is converted to a given raw gas compound Z_i (Eq. (B2)). The fuel flow to the gasifier, $\dot{m}_f$, is calculated from the amount of carbon in the outgoing flows, $\dot{m}_{C,PG}$ and $\dot{m}_{C,FG}$, (measurement points P4 and P5), the amount of carbon in the RME, $\dot{m}_{C,RME}$, and the fraction of carbon in the fuel, $Y_{C,f}$:

$$\dot{m}_f = \frac{\left(\dot{m}_{C,PG} + \dot{m}_{C,FG} - \dot{m}_{C,RME}\right)}{Y_{C,f}}. \qquad (2)$$

The reactions considered for the fuel conversion in the DFB gasifier are summarised in Table VIII, where the subscripts *f*, *v*, *ch*, *syn, i* and *RG* indicate the fuel, volatile matter, char, syngas from char gasification, the generic raw gas compound and the dry raw gas flow, respectively. Furthermore, *n* represents the molar yields of the generic $C_pH_qO_k$ compound on a dry ash-free fuel basis (mol/kg_{daf}); Y_{ch} is the char yield (kg_{char}/kg_{daf}); *a*, *b*, *c* and *d* indicate the stoichiometric reaction coefficients; and $\bar{n}_{O,f,v,ch}$ are the moles of oxygen for stoichiometric combustion of the fuel, char and volatiles, respectively. The decomposition of the biomass in the gasifier is depicted in the Supporting Information (Figure S1), where the fraction X_g of the char yield (Y_{ch}) is converted by R2 (gasification), the fraction λ_{ch} is combusted by the oxygen transport (R3) and the fraction ($1 - X_g$) is transported to the combustor and converted by R6 (combustion), where λ_a describes the excess of air in the reactor. The conversion of volatile matter is described by R4 and R5. In each R4, a fraction Z_i of the volatile matter is converted to one component of the raw gas that contributes to the heating value of the gas, described by the generic molecule $C_pH_qO_k$, and the reaction is balanced with water and carbon dioxide. A fraction of the volatiles λ_v (Eq. (B5)) is combusted by the oxygen transport according to R5. The total oxygen

transport is described by λ_{Otr} (Eq. 6) as the stoichiometric ratio of the oxygen transported to the gasifier and reacting with the fuel (i.e. present in the raw gas) to the oxygen used for stoichiometric combustion of the fuel.

The mass balance equations include the carbon balance (Eq. (B7)) and the balance of volatiles (Eq. (B8)) (Table S2). The fuel conversion is summarised by the fuel conversion variables X_g, λ_{Otr} and Z_i and is used to calculate the internal heat demand of the gasifier [40]. The degrees of freedom of the mass balance equations depend on the available measurements; if the raw gas flow is measured (i.e. the yields of raw gas species are measured) and all the species are detected, the equation has one solution, and the values of X_g, λ_{Otr} and Z_i can be calculated [40]. In particular, the char gasification is calculated from the carbon balance, and the oxygen transport is calculated comparing the oxygen for stoichiometric combustion of the raw gas with that of the fuel at the net of the char to the combustor [40].

In the GoBiGas plant, the flow measurements are available, and the fuel conversion variable can be calculated with a relatively low degree of uncertainty. Other sources of uncertainty, such as measurement errors, fuel composition and raw gas characterisation, are assessed by stochastic simulation of the mass balance inputs, that is, the experimental data. The measurements (including the flows, concentrations, temperatures, fuel composition and tar yields) are varied within a range that is twice the standard deviation (SD) of their measurements according to normal distributions. For each variation of the input, the fuel flow is re-calculated, and the mass balance is solved. The solutions are considered valid if the calculated values of X_g, λ_{Otr} and Z_i are within physically possible ranges, and the fraction of carbon detected by the measurement is lower than the level of carbon in the fuel [40]. The final results are presented as a mean value and SD calculated from the set of valid solutions.

Energy balance of the dual fluidised bed system

The streams considered and the control volumes used for the energy balance of the DFB system are depicted in Figure 3. In contrast to Figure 2, a solution of water and potassium is added to activate the bed material, and the water content in the RME flow to the combustor is $40\%_{vol}$; these features are relevant for the energy balance, while they can be neglected for the carbon balance. The energy balance can be calculated for either the entire DFB system or for each of the reactors using Eqs. (C1)–(C3) (Table S3).

In the assessment of the GoBiGas gasifier, one of the main unknowns is the heat losses $Q_{l,tot}$, which in the GoBiGas plant are considerable because of its relatively small size. The ratio of the heat losses between the combustor $Q_{l,comb}$ and the gasifier $Q_{l,gasif}$ was previously estimated to be 3 [42], based on the external surface and the temperatures of the reactors.

In the scheme reported in Figure 3, the electricity introduced into the system is located in the gasifier, reducing the internal heat demand of the gasifier and the re-circulation of bed material. Nevertheless, the energy balance equations can be easily re-formulated to introduce electricity into the combustor (increasing the re-circulation of bed material).

The energy balance of the gasifier reactor (Eq. (C2)) enables the calculation of the internal heat demand of the gasifier Q_{iHD}, which is used in the simulation to calculate the fraction of product gas that has to be re-circulated to the combustor. Equations 15–17 are used to calculate the

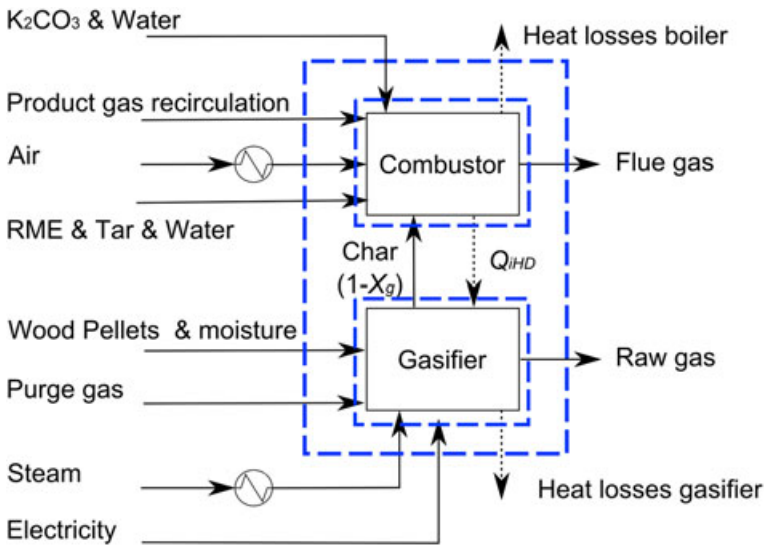

Figure 3. Energy balance of the dual fluidised bed (DFB) system. RME, rapeseed methyl ester. [Colour figure can be viewed at wileyonlinelibrary.com]

heat balance of the gasifier during the extrapolation to new conditions.

Simulation of the dual fluidised bed gasifier

Five key assumptions are made in the simulation algorithm: (1) the circulation of bed material and the oxygen transport are linearly proportional to the internal heat demand of the gasifier (i.e. the oxidation level of the bed material from the combustor is equal for all cases); (2) the RME flow is linearly proportional to the mass flow of the wet raw gas; (3) the average re-circulated flow gas should at a minimum be 1% of the fuel input, to cope with process fluctuations, such as variations in the moisture content; (4) the char gasification can be increased beyond the measured level when the product gas re-circulation is at the minimum level; and (5) the BTX are separated and fed to the combustor. The char gasification depends on several process parameters and on the heat balance of the DFB gasifier. If the heat demand in the combustor is reduced, by, for example, reduced heat losses, the raw gas re-circulation will be reduced.

When the raw gas re-circulation is at the minimum level, the temperature in the gasifier will start to rise, increasing the rate of char gasification. As gasification is endothermal, it moderates the increase in temperature. Through assumption 4, it is assumed that char gasification can be varied within a range (±10 percentage points, pp) and it is calculated from the energy balance while maintaining the temperatures in the reactors. Figure S3 shows the variations of the product gas re-circulation and char gasification used in the simulation algorithm. The first action that can be taken to address a decrease in internal heat demand is to reduce re-circulation of the product gas to the combustor to the minimum level, set according to the need to cope with variations in the process via a rapid regulatory measure. Beyond this point, any further reduction of the heat demand can be compensated by an a reduction of char combustion, making more char available for gasification depending on the design and operational conditions of the gasifier.

In contrast, when the heat demand of the gasifier is increased (e.g. higher moisture content of the fuel), the product gas re-circulation is increased to maintain constant the conditions in the gasifier, including the char gasification. The structure of the simulation algorithm is shown in Figure 4, in which each simulation is defined by a set of independent variables and requires a set of initial values The starting values are initially guessed and thereafter re-calculated through two iterative calculations, one linked to the mass and energy balances of the gasifier to derive λ_{Otr} (step 3) and one linked to the mass and energy balances of the entire system to derive X_g (step 6). Assumption 1, which is concerned with the oxygen transport, and assumption 2, concerning the RME flow, are introduced in steps 3 and 4 of the algorithm, respectively, while assumption 3, which considers re-circulation of the product gas, and assumption 4, which constrains char gasification, are applied in step 6.

To simulate a different chemistry in the reactor, the Z_i values are modified based on the measured composition of the product gas when sulfur is added to the process (Table IX). The distribution of Z_i values is adjusted to match the raw gas composition, assuming that the differences in the concentrations of the measured compounds are related to different rates of conversion of the volatile. Furthermore, the ratio between the C_2H_x and C_3H_x hydrocarbons (not measured) and methane was set as being equal to that of the reference case.

RESULTS AND DISCUSSION

Evaluation of the Gothenburg Biomass Gasification gasifier

The results of the assessment of the DFB gasifier in the GoBiGas plant are reported in Tables X and XI, which show the fuel conversion variables with their associated uncertainties; the results are based on operation using wood pellets as the fuel, with 870 °C as the operating temperature in the gasifier, and potassium-activated olivine as the bed material. The char gasification is 53.8% with an SD of 4.7 pp, and the oxygen transport, λ_{otr}, is estimated as 4.9% (SD, 2.7 pp) of the volume of oxygen required for stoichiometric combustion of the fuel. Calculation of the conversion of volatiles shows that 34.1% of the volatile matter is directly converted to methane, which is favourable for the downstream synthesis processes. The percentages of volatiles converted through the reactions forming tar and BTX are 3.5% and 5.8%, such that in total, 9.3% of the volatiles form unwanted hydrocarbons.

The heat loss of the system, calculated based on the heat balance, corresponds to 5.2% of the energy in the fuel, or about 1.6 MW, of which 0.4 MW is from the gasification side and 1.2 MW is from the combustion. Compared with the heat lost in a typical circulating fluidised bed combustor, which is around 1–2% of the energy of the fuel, the energy lost to the surroundings in the GoBiGas system is considerably higher.

These results highlight the need for better insulation of the reactors, so as to increase the efficiency of the system. The high heat losses affect the energy balance between the two reactors, requiring a high level of re-circulation of the product gas, $E_{PG,rec}$, to maintain the temperature of the process, corresponding to 9.8% of the fuel LHV on a dry basis. The total heat demand of the GoBiGas gasifier is 18% of the energy of the ingoing fuel, whereby about half of the heat demand is covered by the re-circulated gas.

The raw gas efficiency of the gasifier is calculated as 87.3%LHV_{daf} (SD, 1.9 pp), with 71.7%LHV_{daf} (SD, 1.8 pp) of the energy in the fuel being converted into permanent gases and delivered to the methanation section (herein referred to as the 'cold gas efficiency'). Including the energy input from the RME, the efficiency of the

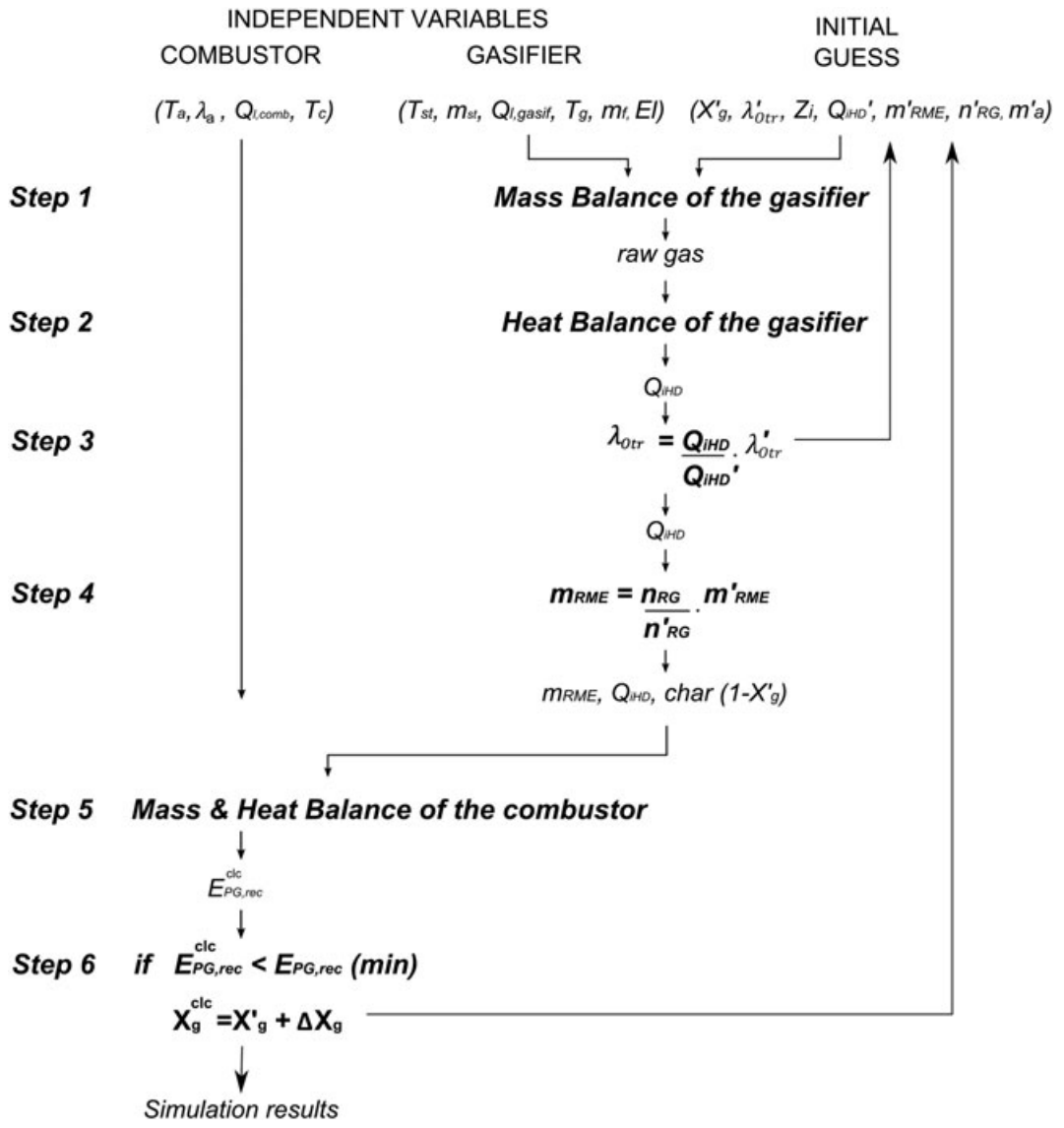

Figure 4. Simulation algorithm.

Table IX. Concentrations of permanent gases and tar following sulfur addition to processes at high and low temperatures

	K,S-act		*K,S-act LT*	
Gasification temperature (°C)	870		820	
Combustion temperature (°C)	920		870	
Measurement point	P1	P3	P1	P3
	Mean	Mean	Mean	Mean
H_2 (vol%$_{dry}$)	n.a.	42.1	n.a.	39.9
CO (vol%$_{dry}$)	n.a.	24.1	n.a.	24.0
CO_2 (vol%$_{dry}$)	n.a.	23.5	n.a.	19.9
CH_4 (vol%$_{dry}$)	n.a.	7.7	n.a.	8.6
Tar (g/Nm^3)	10	6.6	20	13

n.a., not available.

Table X. Mass balance results, X_g, char gasification, Z_i, and volatile matter converted to the *i*-th compound

Parameter (%$_{mass}$)	Mean	SD
X_g	53.8	4.7
λ_{otr}	4.9	2.7
λ_{ch}	0.9	0.5
λ_v	7.8	3.8
Z_{H2}	25.2	1.2
Z_{CO}	9.8	0.8
Z_{CH4}	34.1	0.2
Z_{C2H4}	13.8	0.1
Z_{C3H6}	0.02	0.0
Z_{tar}	3.5	0.2
Z_{btx}	5.8	0.3

Table XI. Energy balance results

	Mean	SD
η_{RG} (%LHV$_{daf}$)	87.3	1.9
η_{CG} (%LHV$_{daf}$)	71.7	1.8
η_{bCH4} (%LHV$_{daf}$)	61.8	1.5
η_{sect} (%)	69.2	1.6
η_{plant} (%)	57.7	1.3
Q_{iHD} (%LHV$_{daf}$)	18	1.0
$E_{PG,rec}$ (%LHV$_{daf}$)	9.8	0.2
$Q_{l,tot}$ (%LHV$_{daf}$)	5.2	0.6
Fuel feed (kg$_{daf}$/h)	5820	142

gasification section is 69.2%E_{tot} (SD, 1.6 pp). The biomethane efficiency, η_{bCH4}, is calculated as 61.8% LHV$_{daf}$ (SD, 1.5 pp), and the plant efficiency, η_{plant}, including all the energy inputs (biomass, electricity and RME) is 57.7%E_{tot} (SD, 1.3 pp) based on the LHV.

Improvements based on the heat demand of the Gothenburg Biomass Gasification gasifier

The sensitivity analysis of the performance of the GoBiGas gasifier aims to identify efficient measures that could be used to improve the efficiency of DFB gasifiers using the GoBiGas gasifier as reference. For this purpose, the air and steam pre-heating, the moisture content of the fuel, the heat losses of the system, the use of sulfur as an additive and the introduction of electricity as a heat source were varied, as described in Simulation of the dual fluidised bed gasifier section, and the results are presented in Figures 5 and 6. The results are expressed as the raw gas efficiency η_{RG}, cold gas efficiency η_{CG}, gasification section efficiency η_{sect} and product gas; the filled markers indicate the relevant reference points from GoBiGas (*K-act* case). Because all of these measures influence the heat demand in the boiler, they affect the required re-circulation of the product gas, as well as the efficiency of the gasification section. Note that as soon as the level of re-circulated product gas reaches the defined minimum, char gasification is increased to fulfil the heat balance, as described in Simulation of the dual fluidised bed gasifier section, and this in turn increases the raw gas efficiency. Because the GoBiGas plant requires a high level of re-circulation of the product gas, owing to the considerable heat losses, most of the measures analysed affect only the re-circulation. Therefore, the only situation in which it is possible to derive a benefit from the significantly increased char gasification is when there is extensive introduction of electricity. Air and steam pre-heating from 300 to 550 °C (Figure 5a) reduces the re-circulation of product gas to about 50% of the reference case, increasing the cold gas efficiency from 71.7%LHV$_{daf}$ to 77.3%LHV$_{daf}$. The reduction of heat losses has an effect similar to that of pre-heating, although the heat losses would need to be reduced by a factor of 5 to increase the η_{CG} to 77.4% LHV$_{daf}$ (Figure 5c). The moisture content depends on the fuel (wood pellets and wood chips) that is being used and the drying process, which is dictated by the economics of the plant, considering both the operational and investment costs for a drying system. A shift from wood pellets (8% moisture) to fresh wood chips (40% moisture, assuming the same chemical composition as the wood pellets) has the effect of reducing η_{CG} from 71.7%LHV$_{daf}$ to 56.3% LHV$_{daf}$ in the current design, while further drying of the fuel to 2% moisture can raise the cold gas efficiency by ~2 pp (Figure 5b). This condition of extreme drying can be achieved with steam dryers, which are connected directly to the feeding system of the DFB gasifier, as suggested previously [31,32]. This type of dryer also pre-heats the biomass to a temperature of 80–100 °C, which further reduces the heat demand in the gasifier [21,32].

Activation with potassium and sulfur affects the gas composition and reduces the tar content, enabling operation of the gasifier across a wider range of conditions. Figure 5d shows the results for the *K,S-act* case with low tar content and the same temperature levels as in the *K-act* case (Table IX) and for the *K,S-act LT* case with the same tar content as the base case, but with the temperature in the reactors reduced by 50 °C (Table IX). In the *K,S-act* case, the lower yield of tar indicates that more energy is stored in the permanent gas, although this is partially compensated for by the higher level of re-circulation of the product gas, which is used to counteract the lower tar flow to the combustor. In the *K,S-act LT* case, the lower temperature in the reactor reduces both the heat demand in the combustor and the product gas re-circulation, while the tar yield is similar to that in the base case. Overall, the cold gas efficiency is increased to 72.9%LHV$_{daf}$ for the *K, S-act* case and to 74.2%LHV$_{daf}$ for the *K,S-act LT* case.

The introduction of electricity into the DFB gasifier affects multiple aspects of the process. Overall, the re-circulation of the product gas is reduced, and it may reach the minimum value (Figure 6). If more electricity is provided, the gasification of char may increase. Using electricity as a heat source in the gasifier reactor improves the rate of fuel conversion, that is, the raw gas efficiency (Figure 6). Initially, this is due to the reduced rate of oxygen transport, whereas later, it is due to the higher level of char gasification. The minimum level of re-circulation of product gas in this case is reached by introducing electricity for 8% of the energy in the fuel, thereby achieving a cold gas efficiency of 82.1%LHV$_{daf}$. An electricity input corresponding to 10% of the LHV of the fuel would enable char gasification to be increased from 53.8% to 60% and would increase the raw gas efficiency to 92.3%LHV$_{daf}$. Unlike the other measures investigated, the introduction of electricity causes the cold gas efficiency and the efficiency of the gasification section to diverge in Figure 6, because in the latter, the electricity is accounted for as an energy input. In particular, for the case in which electricity replaces 8% of the LHV of the fuel, the efficiency of the gasification section increases by ~4.5 pp, while the cold gas efficiency is increased by ~10 pp. The effects of the electricity on the overall plant (power-to-gas efficiency) in combination with the measures described

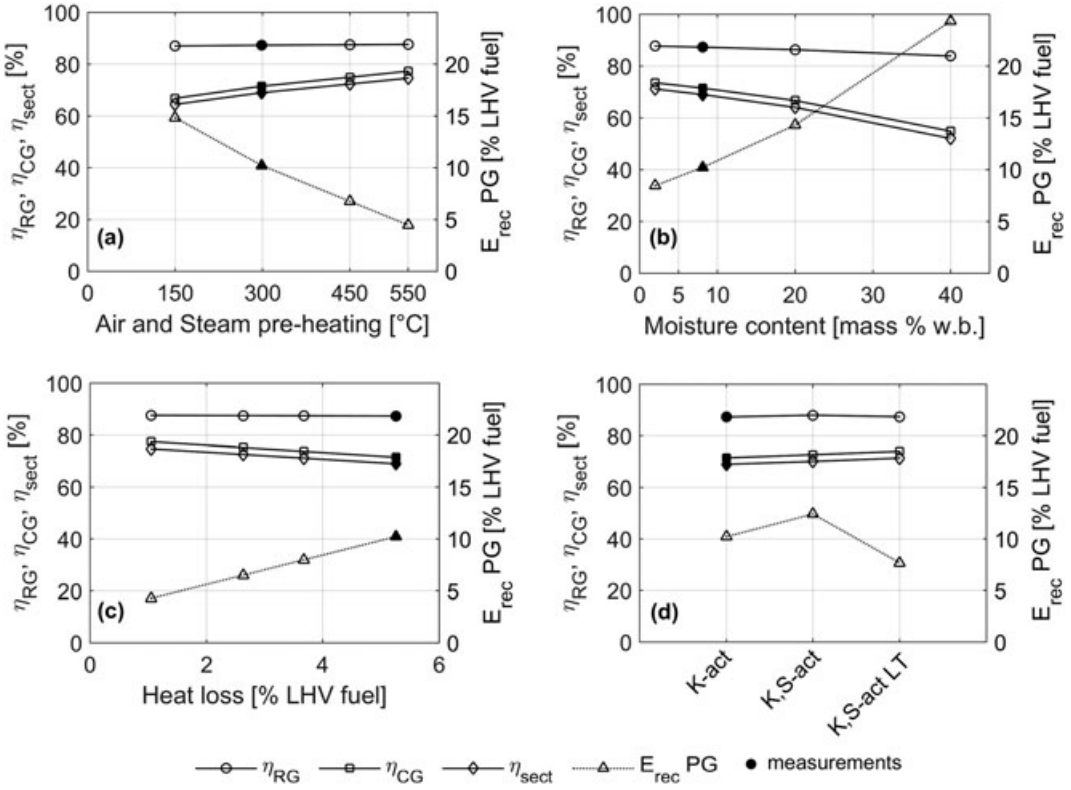

Figure 5. Sensitivity analysis of thermal measures.

previously are investigated in Case study: performance of a commercial-scale gasification plant section.

Case study: performance of a commercial-scale gasification plant

The combined effect of improved thermal measures is investigated with a view to possible designs for a large-scale plant. The results are shown in Figure 7 and Table XII for both dried woody biomass (e.g. pellets or very dry wood chips; 8% moisture w.b.) and fresh wood biomass (e.g. wood chips or forest residues; 40% moisture w.b.). The cases investigated included the (1) *K-act* base case; (2) *K,S-act LT* with addition of sulfur; (3) *K,S-act* with addition of sulfur and low operational temperature; (4) *K,S-act LT, PH* and *Ql* with sulfur addition and low operational temperature, with pre-heating up to 550 °C and heat losses reduced by a factor of 3; (5) *K,S-act LT, PH, Ql* and *El*; and (6) *K,S-act LT, PH, Ql* and El_{int}, the latter two of which introduce electricity from the grid and electricity that is produced internally from heat recovery, respectively. In Figure 7, the results for the DFB gasifier and the biomethane production process are expressed in terms of the cold gas and biomethane efficiencies (based on the LHV of the fuel), as well as the efficiencies of the gasification section and the plant, which include all the energy inputs. In the calculation of the plant efficiency η_{plant}, electricity is included among the energy inputs if it is obtained from the grid and excluded if it is produced locally from waste heat. Electricity is always considered to be an external energy input for the efficiency of the gasification section η_{sect}. A summary of the results for all the cases is reported in Table XII. A comparison of the *K-act* and *K,S*-act *LT* cases shows how the lower temperature achieved in the reactors by sulfur addition leads to increases in η_{CH4} and η_{plant} of about 1 pp, for both dried woody biomass and fresh wood chips. Thus, the

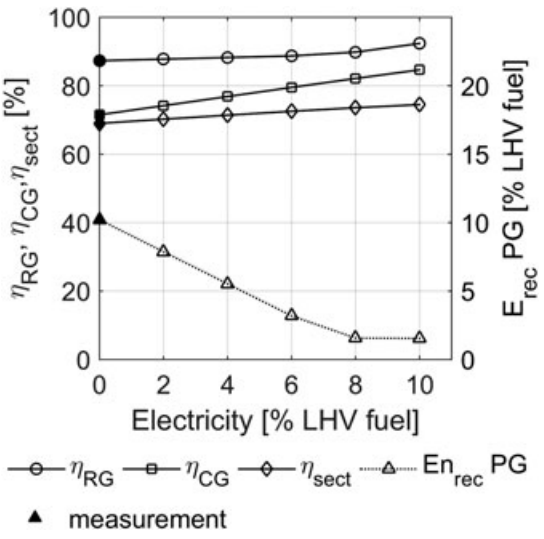

Figure 6. Effects of electricity introduction into the gasifier reactor.

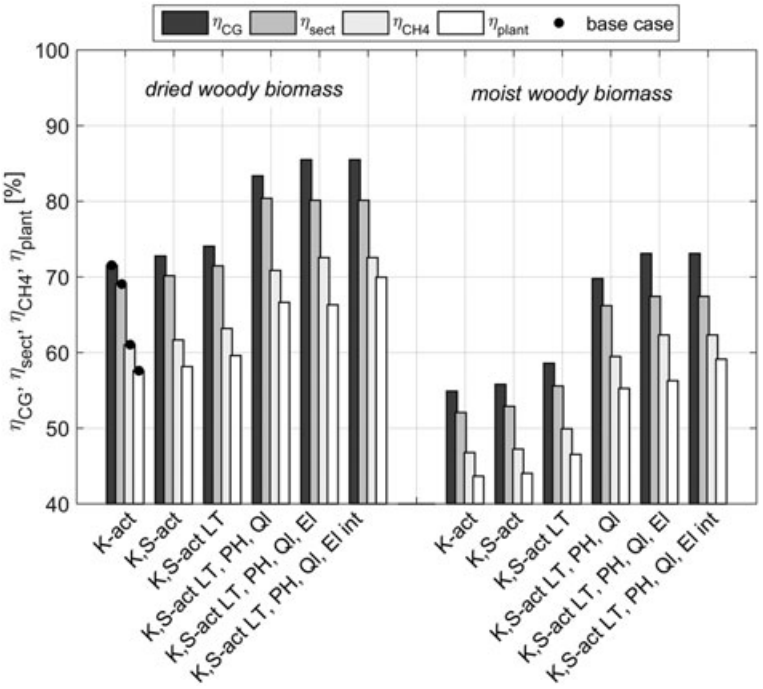

Figure 7. Simulation of the process design cases and efficiencies.

addition of sulfur to the DFB gasifier produces considerable benefits, not only in reducing the operational problems associated with tar clogging but also in significant increases in the efficiencies. With sulfur addition and a lower temperature, the GoBiGas plant achieves a biomethane efficiency of 63.3%LHV_{daf}, approaching the 65%LHV_{daf} target of the project. For the cases of *K,S-act LT, PH* and *Ql*, Figure 7 shows that the combined effect of sulfur addition, extended pre-heating and better insulation of the reactors achieves a biomethane efficiency of 71%LHV_{daf} with dried biomass and 60.5%LHV_{daf} using moist biomass. Compared with the reference case, GoBiGas, the increases in the levels of the cold gas efficiency using wood pellets and fresh wood chips are approximately 11 (83.5%LHV_{daf}) and 14 pp (71%LHV_{daf}), respectively. With this design (*K, S-act LT, PH* and *Ql*), re-circulation of the product gas is reduced to the minimum, whereas char gasification is not increased.

The electricity introduced to the gasifier, in the two cases of *K,S-act LT, PH, Ql* and *El*, and *K,S-act LT, PH, Ql* and El_{int}, corresponds to 3% of the LHV of the fuel and is in the same order of magnitude as the power consumption of the plant (3.75%LHV_{daf}). The total electricity consumption (6.75%LHV_{daf}) is compatible with the electricity production from heat recovery in a large plant, estimated as 3–10% of the energy of the fuel [43]. The results show that by introducing electricity, it is possible to increase the raw gas efficiency when using dried biomass to 94.4%LHV_{daf}, corresponding to a char gasification fraction of 61%. Thus, to achieve this performance, the rate of char gasification should be increased beyond the rate currently obtained at the GoBiGas gasifier.

Several parameters that influence char gasification have been identified, including the catalytic effects of additives and bed materials, residence time, mixing of char in the multiphase flow and temperature. However, the correlations between these parameters and the level of gasification are not fully understood, and there is potential to achieve further improvements in the efficiency of gasification.

When electricity is used in combination with moist biomass, most of the electricity compensates for the higher rate of moisture evaporation in the gasifier. Therefore, the rate of product gas re-circulation is minimised, with a small increase in char gasification and a cold gas efficiency that corresponds to 75%LHV_{daf}. The efficiency of biomethane production is 74.3%LHV_{daf} with dried biomass and 64.0%LHV_{daf} with moist biomass. The plant efficiency is affected by the origin of the electricity, that is, whether it is produced from waste heat or obtained from the grid. In the latter case, the η_{plant} is estimated as 68.2%E_{tot} with dried biomass and as 58.7%E_{tot} with moist biomass. Because of the high-level efficiency of the gasification process, the conversion of electricity to methane is more efficient than current state-of-the-art power-to-methane processes, which employ an electrolyser and further synthesis of hydrogen with renewable CO_2 [44–47]. The efficiency of current state-of-the-art power-to-methane processes is in the range of 45–50% based on LHV [44,45,48] with aims to achieve 55–63% based on LHV

Table XII. Summary of the process efficiencies based on dry ash-free and a.r. biomass (50% moisture), for biomass moisture contents of 40%, 8% and 2% moisture w.b., respectively

		Energy inputs		Efficiencies on LHV_{daf} (%)					Efficiencies on LHV a.r. fresh[§] (%)				
		Rapeseed methyl ester (%MJ_{fuel})	EI_{tot} (%MJ_{fuel})	η_{RG}	η_{CG} (%LHV_{daf})	η_{bCH4}	η_{sect} (%E_{tot})	η_{plant}	η_{RG}	η_{CG} (%$LHV_{a.r.}$)	η_{bCH4}	η_{sect} (%E_{tot})	η_{plant}
Extremely dried wood*	K_{act}	3.3	3.75	87.7	73.6	62.8	71.2	59.4	100.9	93.9	72.2	81.5	67.7
	K, S_{act}	3.3	3.75	88.4	74.8	63.4	72.3	59.9	101.7	98.1	73.0	82.8	68.4
	K, S_{act} *LT*	3.3	3.75	87.8	75.9	64.8	73.4	61.2	101.0	94.0	74.5	84.1	69.9
	K, S_{act} *LT, PH, QI*	3.3	3.75	92.6	85.0	72.1	82.1	67.9	106.5	99.5	83.0	94.0	77.5
	K, S_{act} *LT, PH, QI, EI*[¶]	3.3	6.75	95.9	88.3	75.4	82.9	69.2	110.4	103.3	86.8	94.5	77.7
	K, S_{act} *LT, PH, QI,* EI_{int}[¶]	3.3	0.0	95.9	88.3	75.4	82.9	71.2	110.4	103.3	86.8	94.5	82.7
Dried wood[†]	K_{act}	3.3	3.75	87.3	71.7	61.1	69.2	57.7	100.5	93.5	70.3	79.2	65.9
	K, S_{act}	3.3	3.75	88.0	72.9	61.8	70.3	58.2	101.2	97.6	71.1	80.4	66.4
	K, S_{act} *LT*	3.3	3.75	87.3	74.2	63.3	71.6	59.7	100.6	93.6	72.8	81.9	68.1
	K, S_{act} *LT, PH, QI*	3.3	3.75	91.1	83.5	71.0	80.5	66.7	104.8	97.8	81.7	92.2	76.1
	K, S_{act} *LT, PH, QI, EI*[¶]	3.3	6.75	94.4	87.6	74.3	82.2	68.2	108.6	102.6	85.5	93.6	77.1
	K, S_{act} *LT, PH, QI,* EI_{int}[¶]	3.3	0.0	94.4	87.6	74.3	82.2	70.2	108.6	102.6	85.5	93.6	82.0
Moist wood[‡]	K_{act}	3.3	3.75	84.1	56.3	48.0	53.4	44.7	96.7	90.1	55.2	61.0	51.0
	K, S_{act}	3.3	3.75	84.7	57.2	48.4	54.2	45.1	97.5	94.1	55.7	61.9	51.4
	K, S_{act} *LT*	3.3	3.75	84.2	59.9	51.0	56.8	47.6	96.9	90.3	58.7	64.9	54.2
	K, S_{act} *LT, PH, QI*	3.3	3.75	84.9	71.0	60.5	67.4	56.2	97.6	91.0	69.6	76.9	64.0
	K, S_{act} *LT, PH, QI, EI*[¶]	3.3	6.75	85.6	75.0	64.0	69.3	58.7	98.5	92.6	73.6	78.8	65.6
	K, S_{act} *LT, PH, QI,* EI_{int}[¶]	3.3	0.0	85.6	75.0	64.0	69.3	60.5	98.5	92.6	73.6	78.8	69.3

a.r., as-received.
*Case with 2% moisture w.b.
[†]8% moisture w.b.
[‡]40% moisture w.b.
[§]50% moisture w.b.
[¶]Electricity provided to exchange for 3%LHV_{daf} in the gasifier reactor.

Int. J. Energy Res. (2017) © 2017 The Authors. *International Journal of Energy Research* published by John Wiley & Sons Ltd.
DOI: 10.1002/er

[49–51] with the development of high temperature electrolysis cells, as comparison, a plant efficiency of 55–65%E_{tot} is already achievable with the GoBiGas technology. Therefore, the direct utilisation of electricity as the heat source in the gasifier represents a viable option for a high-efficient power-to-methane process.

Another measure of efficiency when using electricity to enhance the biomethane process is the power-to-gas efficiency (η_{P2G}, Table VII). The power-to-gas efficiency is depended on the reference process used in the calculation because the heat provided can be used either to reduce the combustion of product gas or char (increasing gasification). When product gas re-circulation is substituted by electricity, η_{P2G} is ~85% and gradually increases to values above 105%, if the electricity converted is stored as chemical energy in the gasification products (i.e. char gasification is increased).

For the case with electricity that is produced locally (i.e. *K,S-act LT, PH, Ql* and El_{int}), it is assumed that the level of production corresponds to the total electricity demand of the plant. The biomethane efficiency corresponds to that of the *K,S-act LT, PH, Ql* and *El* case, while the plant efficiency is 71.7% or 61.1% higher with wood pellets or wood chips as the fuel, respectively. These efficiency levels are considerably higher than the current efficiency level of the GoBiGas plant.

The efficiencies presented in the results are based on the LHV of the dry ash-free fuel. Nevertheless, it is common practice on the European biomass market to use LHV based on the as-received fuel for establishing prices. As a comparison with the data from the literature, Table XII summarises the efficiencies of all the plant designs based on the LHVs of both dry ash-free biomass and as-received fresh biomass, with 50% moisture, which corresponds to the moisture content of biomass in the northern hemisphere directly after harvesting.

Table XII also includes a simulation of an intensively dried biomass (2% moisture w.b.), which can be achieved using steam dryers [31,32]. The three biomass cases with different moisture contents (2%, 8% and 40% moisture w.b.) are presented to demonstrate the benefit of investing in a biomass dryer upstream of the gasifier. Using the *K,S-act LT* design as reference, the value of η_{bCH4} based on the LHV of fresh biomass (50% moisture) is increased from 58.7% with natural drying at the storage site (40% moisture w.b.) to 72.8% with dried biomass (8% moisture w.b.), and finally to 74.5% with extensively dried biomass (2% moisture w.b.). Therefore, the benefit of drying the biomass is such that should justify the installation of a drying system.

CONCLUSIONS

The mass and heat balance of the gasification section in the GoBiGas plant were evaluated from the data collected in the first experimental campaign. The efficiency of biomass conversion in the GoBiGas gasifier was evaluated during an experimental series with potassium-activated olivine as the bed material and dried woody biomass (pellets with 8% moisture w.b.) as the fuel. Char gasification in the gasifier was 53.8% (SD, 4.7 pp), yielding a raw gas efficiency of 87.3%LHV_{daf} (SD, 1.9 pp). The fraction of volatile mass converted directly to methane was 34.1%$_{mass}$ (SD, 0.2), which is considered favourable for the biomethane process. The level of fuel conversion ensures high efficiency of the biomethane process, although because of the limitation associated with the design of a relatively small-scale unit, the high heat losses limit the cold gas efficiency. From the heat balance, the heat losses were calculated as 5.2% (SD, 0.6 pp) of the fuels LHV, which is higher than the reference values for biomass boilers. The heat losses were compensated by the combustion of product gas, yielding a cold gas efficiency of 71.7%LHV_{daf} (SD, 1.8 pp).

The activation of the bed material by potassium and sulfur has extended the operational range of the gasifier by reducing the yields of tar, or by enabling operation at lower temperatures. Both these conditions were investigated. The low-temperature case revealed up to 2.5 pp higher cold gas efficiency than the reference case (potassium-activated case), while maintaining the temperature and reducing the tar yield increased the cold gas efficiency by 1.2 pp. Therefore, decreasing the operational temperature while enhancing activation of the bed material with sulfur is an efficient approach to increasing the efficiency of a DFB gasifier. The biomethane efficiency achieved using potassium-sulfur activation and a reduced temperature was 63.3%LHV_{daf}, which approaches the project target of 65%LHV_{daf}, when using dried biomass (8% moisture).

The sensitivity analysis on the GoBiGas gasifier shows that reducing heat losses (to 1% of the energy of the fuel) and increasing pre-heating to 550 °C have the potential to increase the cold gas efficiency by 3 and 6 pp, respectively. These measures combined with a lower operational temperature through activation of the bed material with potassium and sulfur increase the cold gas efficiency to 83.5%LHV_{daf}, which is feasible with existing technologies and represents the state of the art for DFB gasifiers operated with dried biomass (8% moisture w.b.). The biomethane efficiency in these conditions is 71%LHV_{daf}, which is considerably higher than the GoBiGas target.

The penalty associated with using fresh biomass (40% moisture w.b.) rather than dried biomass (8% moisture w.b.) is approximately 16 pp for the cold gas efficiency and 14 pp for the biomethane efficiency, because of the increased combustion of product gas. The benefit of biomass drying prior to gasification was quantified by re-calculating the efficiency on the basis of the LHV as-received of the harvested biomass (50% moisture w.b.), which is used in the trades. Drying to 40%, 8% and 2% moisture contents results in biomethane efficiencies of 55.2%$LHV_{50\%}$, 70.3%$LHV_{50\%}$ and 72.2%$LHV_{50\%}$, respectively. Therefore, drying is crucial for the performance and economics of the plant.

A power-to-methane concept for the conversion of electricity to biomethane by direct heating of the gasifier reactor was evaluated, showing high-potential efficiency. The efficiency of the power-to-methane conversion can reach values as high as 105% (η_{P2G}), in an optimised process where the electricity provides heat to increase the gasification reaction. The overall efficiency of the process, including the electricity converted to methane, is in the range of 68.2%E_{tot} and 58.7%E_{tot} for the dried and moist biomasses, respectively. These efficiencies are significantly higher than those of power-to-methane processes based on electrolysis (rated in the range of 45–55% based on LHV). Therefore, biomass gasification can also play a major role in the conversion of intermittent electricity sources to renewable biofuels.

To explore the potential of a highly optimised stand-alone plant, a design with conversion of electricity that is locally produced at the plant was evaluated. Assuming that the electricity demand of the plant (3.75% of the energy of the fuel) and the electricity sent to the gasifier (3% of the energy of the fuel) are produced from the excess heat in the process, the efficiency of the process is increased to 70.2%E_{tot} with dried biomass (8% moisture) and 60.5% E_{tot} with moist biomass (40% moisture). This option is suitable for large plants (>100 MW_{fuel}), where the installation of a steam cycle is an economically viable option. To achieve higher levels of efficiency, it is necessary to dry further, pre-heat the fuel and lower the operating temperature.

In summary, the fuel conversion and the efficiency in the gasification section of the GoBiGas plant were estimated, revealing the strong potential of dual fluidized bed gasification for large-scale production of advanced biofuels. The data provided represent the first real reference, from a commercial scale plant, at support of the numerous investigations on techno-economic analysis and modelling of energy system.

NOMENCLATURE

Symbols	Unit	Description
a, b, c, d	mol/kg_{daf}	Stoichiometric coefficients
El	MJ_{el}/h	Electricity to the DFB gasifier
El_{tot}	MJ_{el}/h	Total electricity demand in the plant
E_s	MJ/h	Chemical energy in the *s*-th stream calculated from the LHV
H_s	MJ/h	Enthalpy term for the *s*-th stream
$\dot{m}_f$	kg_{daf}/h	Fuel feed to the gasifier
$\dot{m}_{C,PG}$	kg_{daf}/h	Carbon flow in the product gas
$\dot{m}_{C,FG}$	kg_{daf}/h	Carbon flow in the flue gas
$\dot{m}_{C,RME}$	kg_{daf}/h	Carbon flow in the RME
$n_{C,H,O}$	mol/kg_{daf}	Molar yield of the C, H and O
$n_{C,(ch,v,\ rg)}$	mol/kg_{daf}	Molar yield of the carbon in char, volatile and raw gas
$-n_{O,(f,ch,v)}$	mol_O/kg	Stoichiometric oxygen for combustion
η_{RG}	MJ/MJ_{fuel}	Raw gas efficiency
η_{CG}	MJ/MJ_{fuel}	Cold gas efficiency
η_{bCH4}	MJ/MJ_{fuel}	Cold gas efficiency
η_{sect}	MJ/MJ_{tot}	Gasification section efficiency
η_{plant}	MJ/MJ_{totl}	Plant efficiency
η_{P2G}	MJ_{bCH4}/MJ_{el}	Power-to-gas efficiency
Q_{iHD}	MJ/kg_{daf}	Internal heat demand of the gasification reactor
$Q_{l,tot,(comb)}$	MW	Heat losses total and combustor
$Y_{C,f}$	kg_C/kg_{daf}	Carbon yield in the fuel
λ_a	–	Air-to-fuel equivalence ratio
λ_{Otr}	mol_{Otr}/$mol_{O,f}$	Total oxygen transport equivalence ratio
λ_{ch}	mol_{Otr}/$mol_{O,ch}$	Oxygen transport to char equivalence ratio
λ_v	mol_{Otr}/$mol_{O,ch}$	Oxygen transport to volatiles equivalence ratio
X_g	–	Fraction of char gasified
Z_i	–	Fraction of volatile matter converted to the formation of the *i*-th combustible raw gas compound

Subscripts	Terms	Description
i	H_2, CO, CH_4, C_2H_4, C_3H_6, tar, BTX	Raw gas compounds: H_2, CO, CH_4, C_2H_4, C_3H_6, tar (removed in the RME scrubber), BTX (removed in the carbon beds)
s	*f*, *f a.r.*, *ch*, *v*, *syn*, *i*, *RG*, *PG*, PG_{rec}, *CG*, *OC*, *tar*, *RME*, *a*, *st*, *pur*, RME_{mix}, K_{mix}, *bCH4*	Streams: dry ash-free fuel, fuel as received, char, volatiles, syngas, raw gas compound, raw gas, product gas, re-circulated product gas, cold gas, organic compounds, tar, combustion air, steam, purge gas, RME and water, K_2CO_3 and water, biomethane

(*Continues*)

ACKNOWLEDGEMENTS

This work was supported by Göteborg Energi AB, Metso Power AB and the Competency Center of the Svenskt Förgasningscentrum (SFC), in collaboration with the Swedish Energy Agency.

REFERENCES

1. Cooper BL, London JR, Mellon RJ, Behrens MA. Chapter 4: integrated forest biorefineries: product-based economic factors. In *Integrated Forest Biorefineries: Challenges and Opportunities*. The Royal Society of Chemistry, 2013; 98–116.
2. Lange JP. Lignocellulose conversion: an introduction to chemistry, process and economics. *Biofuels, Bioproducts and Biorefining* 2007; **1**(1):39–48.
3. Foust TD, Aden A, Dutta A, Phillips S. An economic and environmental comparison of a biochemical and a thermochemical lignocellulosic ethanol conversion processes. *Cellulose* 2009; **16**(4):547–565.
4. Zinoviev S, Muller-Langer F, Das P, Bertero N, Fornasiero P, Kaltschmitt M, Centi G, Miertus S. Next-generation biofuels: survey of emerging technologies and sustainability issues. *ChemSusChem* 2010; **3**(10):1106–1133.
5. Demirbas A. Biorefineries: current activities and future developments. *Energy Conversion and Management* 2009; **50**(11):2782–2801.
6. Wang B, Gebreslassie BH, You FQ. Sustainable design and synthesis of hydrocarbon biorefinery via gasification pathway: integrated life cycle assessment and technoeconomic analysis with multiobjective superstructure optimization. *Computers & Chemical Engineering* 2013; **52**:55–76.
7. Sikarwar VS, Zhao M, Clough P, Yao J, Zhong X, Memon MZ, Shah N, Anthony EJ, Fennell PS. An overview of advances in biomass gasification. *Energy & Environmental Science* 2016.
8. Zhang LH, Xu CB, Champagne P. Overview of recent advances in thermo-chemical conversion of biomass. *Energy Conversion and Management* 2010; **51**(5): 969–982.
9. Gunnarsson, I. *The GoBiGas Project*; 2011.
10. Gassner M, Marechal F. Thermo-economic optimisation of the polygeneration of synthetic natural gas (SNG), power and heat from lignocellulosic biomass by gasification and methanation. *Energy & Environmental Science* 2012; **5**(2):5768–5789.
11. Bridgwater AV, Toft AJ, Brammer JG. A techno-economic comparison of power production by biomass fast pyrolysis with gasification and combustion. *Renewable and Sustainable Energy Reviews* 2002; **6**(3):181–248.
12. Kalinci Y, Hepbasli A, Dincer I. Biomass-based hydrogen production: a review and analysis. *International Journal of Hydrogen Energy* 2009; **34**(21):8799–8817.
13. Anex RP, Aden A, Kazi FK, Fortman J, Swanson RM, Wright MM, Satrio JA, Brown RC, Daugaard DE, Platon A, Kothandaraman G, Hsu DD, Dutta A. Techno-economic comparison of biomass-to-transportation fuels via pyrolysis, gasification, and biochemical pathways. *Fuel* 2010; **89**:S29–S35.
14. Brown TR, Brown RC. Techno-economics of advanced biofuels pathways. *RSC Advances* 2013; **3**(17):5758–5764.
15. Berdugo Vilches T, Marinkovic J, Seemann M, Thunman H. Comparing active bed materials in a dual fluidized bed biomass gasifier: olivine, bauxite, quartz-sand, and ilmenite. *Energy & Fuels* 2016.
16. Thunman H, Larsson A, Hedenskog M. *Commissioning of the GoBiGas 20MW Bio-methane Plant, TCBiomass*. Chicago: Chicago, 2015.
17. Burman Å. Experiences from the building and commissioning of the GoBiGas-pl. In SFC confernce, Gothenburg, 2016.
18. Biomass CHP station Senden. http://www.4biomass.eu/en/best-practice/project-biomass-chp-station-senden.
19. Pfeifer C, Hofbauer H. Development of catalytic tar decomposition downstream from a dual fluidized bed biomass steam gasifier. *Powder Technology* 2008; **180**(1–2):9–16.
20. Hofbauer H, Rauch R, Loeffler G, Kaiser S, Fercher E, Tremmel H. In Six years experience with the FICFB-gasification process, 12th European conference and technology exhibition on biomass for energy, industry and climate protection, 2002.
21. Larsson A, Seemann M, Neves D, Thunman H. Evaluation of performance of industrial-scale dual fluidized bed gasifiers using the Chalmers 2–4-MWth gasifier. *Energy & Fuels* 2013; **27**(11):6665–6680.
22. Milne TA, Abatzoglou N, Evans RJ, Laboratory NRE. *Biomass Gasifier "Tars": Their Nature, Formation, and Conversion*. National Renewable Energy Laboratory, 1999.
23. Rauch R, Pfeifer C, Bosch K, Hofbauer H, Swierczynski D, Courson C, Kiennemann A. In Comparison of different olivines for biomass steam gasification, Science in Thermal and Chemical Biomass Conversion, Victoria, Canada, 30th August to 2nd September 2004; Victoria, Canada, 2004.
24. Sutton D, Kelleher B, Ross JRH. Review of literature on catalysts for biomass gasification. *Fuel Processing Technology* 2001; **73**(3):155–173.
25. Campoy M, Gómez-Barea A, Fuentes-Cano D, Ollero P. Tar reduction by primary measures in an autothermal air-blown fluidized bed biomass gasifier.

Industrial and Engineering Chemistry Research 2010; **49**(22):11294–11301.
26. Abu El-Rub Z, Bramer EA, Brem G. Review of catalysts for tar elimination in biomass gasification processes. *Industrial and Engineering Chemistry Research* 2004; **43**(22):6911–6919.
27. Aranda G, van der Drift A, Vreugdenhil BJ, Visser HJM, Vilela CF, van der Meijden CM. Comparing direct and indirect fluidized bed gasification: effect of redox cycle on olivine activity. *Environmental Progress and Sustainable Energy* 2014; **33**(3):711–720.
28. Marinkovic J, Thunman H, Knutsson P, Seemann M. Characteristics of olivine as a bed material in an indirect biomass gasifier. *Chemical Engineering Journal* 2015; **279**:555–566.
29. Kirnbauer F, Wilk V, Kitzler H, Kern S, Hofbauer H. The positive effects of bed material coating on tar reduction in a dual fluidized bed gasifier. *Fuel* 2012; **95**(1):553–562.
30. Larsson A, Hedenskog M, Thunman H. Monitoring the bed material activation in the GoBiGas – gasifier. In *Nordic Flame Days Copenhagen*. 2015.
31. Fagernas L, Brammer J, Wilen C, Lauer M, Verhoeff F. Drying of biomass for second generation synfuel production. *Biomass and Bioenergy* 2010; **34**(9): 1267–1277.
32. Alamia A, Ström H, Thunman H. Design of an integrated dryer and conveyor belt for woody biofuels. *Biomass and Bioenergy* 2015, **77** (0), 92–109.
33. Zhang Y, Gong X, Zhang B, Liu W, Xu M. Potassium catalytic hydrogen production in sorption enhanced gasification of biomass with steam. *International Journal of Hydrogen Energy* 2014; **39**(9):4234–4243.
34. Fahmi R, Bridgwater AV, Darvell LI, Jones JM, Yates N, Thain S, Donnison IS. The effect of alkali metals on combustion and pyrolysis of *Lolium* and *Festuca* grasses, switchgrass and willow. *Fuel* 2007; **86**(10–11):1560–1569.
35. McKee DW. Fundamentals of catalytic coal and carbon gasification mechanisms of the alkali metal catalysed gasification of carbon. *Fuel* 1983; **62**(2):170–175.
36. Wang L, Hustad JE, Skreiberg Ø, Skjevrak G, Grønli M. A critical review on additives to reduce ash related operation problems in biomass combustion applications. *Energy Procedia* 2012; **20**:20–29.
37. Heyne S, Thunman H, Harvey S. Extending existing combined heat and power plants for synthetic natural gas production. *International Journal of Energy Research* 2012; **36**(5):670–681.
38. Gassner M, Maréchal F. Thermo-economic process model for thermochemical production of synthetic natural gas (SNG) from lignocellulosic biomass. *Biomass and Bioenergy* 2009; **33**(11):1587–1604.
39. Alamia A, Gardarsdòttir SÒ, Larsson A, Normann F, Thunmann H. Efficiency comparison of large-scale standalone, centralized and distributed thermochemical biorefineries. *Energy Technology* 2016, n/a-n/a.
40. Alamia A, Thunman H, Seemann M. Process simulation of dual fluidized bed gasifiers using experimental data. *Energy & Fuels* 2016; **30**(5):4017–4033.
41. Kroese DP, Brereton T, Taimre T, Botev ZI. Why the Monte Carlo method is so important today. *Wiley Interdisciplinary Reviews: Computational Statistics* 2014; **6**(6):386–392.
42. Karlbrink M. *An Evaluation of the Performance of the GoBiGas Gasificaiton Process*. Chalmers University of Technology, 2015.
43. Heyne S. *Bio-SNG from Thermal Gasification – Process Synthesis*. Chalmers University of Technology: Integration and Performance, 2013.
44. Götz M, Lefebvre J, Mörs F, McDaniel Koch A, Graf F, Bajohr S, Reimert R, Kolb T. Renewable power-to-gas: a technological and economic review. *Renewable Energy* 2016; **85**:1371–1390.
45. Gahleitner G. Hydrogen from renewable electricity: an international review of power-to-gas pilot plants for stationary applications. *International Journal of Hydrogen Energy* 2013; **38**(5):2039–2061.
46. Ursua A, Gandia LM, Sanchis P. Hydrogen production from water electrolysis: current status and future trends. *Proceedings of the IEEE* 2012; **100**(2):410–426.
47. Parthasarathy P, Sheeba KN. Combined slow pyrolysis and steam gasification of biomass for hydrogen generation – a review. *International Journal of Energy Research* 2015; **39**(2):147–164.
48. Jentsch M, Trost T, Sterner M. Optimal use of power-to-gas energy storage systems in an 85% renewable energy scenario. *Energy Procedia* 2014; **46**:254–261.
49. Zoss T, Dace E, Blumberga D. Modeling a power-to-renewable methane system for an assessment of power grid balancing options in the Baltic States' region. *Applied Energy* 2016; **170**:278–285.
50. Ebbesen SD, Jensen SH, Hauch A, Mogensen MB. High temperature electrolysis in alkaline cells, solid proton conducting cells, and solid oxide cells. *Chemical Reviews* 2014; **114**(21):10697–10734.
51. Nechache A, Cassir M, Ringuedé A. Solid oxide electrolysis cell analysis by means of electrochemical impedance spectroscopy: a review. *Journal of Power Sources* 2014; **258**:164–181.

SUPPORTING INFORMATION

Additional Supporting Information may be found online in the supporting information tab for this article.